

Consideration of the values of the interligand S...S distances shows that the distortion of the MoS_3 core results from the twisting of only one of the three chelating ligands [that containing S(1) and S(2)] toward the octahedral limit; the relative orientation of the other two ligands remains similar to that found in trigonal prismatic structures. A similar unsymmetrical distortion is found³³ in the $[\text{Ta}(\text{bdt})_3]^-$ ion, which has trans angle values of 147.19 (8), 158.09 (8), and 158.69 (8)°, and a dihedral angle between the two S_3 faces of ca. 12°.

It has previously been proposed¹¹ that the trigonal prismatic structure observed for some metal tris(dithiolene) complexes is stabilized by π -bonding interactions between metal-based d orbitals (d_{xy} and $d_{x^2-y^2}$) and sulfur-based p orbitals of the ligands. According to this model, reduction of neutral, formally $\text{Mo}(\text{VI})$ complexes to yield charged anionic species populates the a_1 molecular orbital¹¹ of the complex, which has primarily metal d_z^2 character. Since the π -interaction of the latter metal orbital with the ligands is antibonding in character, this model predicts that more highly reduced complexes should have structures that are more strongly distorted from the trigonal prismatic limit. The structures of the $[\text{Mo}(\text{qdt})_3]^-$ and $[\text{Mo}(\text{qdt})_3]^{2-}$ ions (Table VI) clearly contradict this model, suggesting that steric (crystal packing) effects might play the dominant role in determining the coordination geometry of the anions. In the present study, the $\{\text{Mo}[\text{S}_2\text{C}_2(\text{CF}_3)_2]_3\}^-$ ion is found to be a nearly perfect trigonal prism, while the $\{\text{Mo}[\text{S}_2\text{C}_2(\text{CF}_3)_2]_3\}^{2-}$ ion is distorted, a result that would appear to be in accordance with the above MO description. However, the irregular nature of the distortion and its apparent relation to the crystal packing argues against electronic factors as an explanation. Specifically, it is found that the twisted ligand in the structure of the $\{\text{Mo}[\text{S}_2\text{C}_2(\text{CF}_3)_2]_3\}^{2-}$ ion is the only one involved in face-to-face stacking interactions with the decamethylferrocenium cations, while the remaining two

ligands interact with a neighboring cation in a side-on manner that severely restricts their ability to twist relative to one another. Given the nature of these intermolecular interactions, we conclude that the distortion of the $\{\text{Mo}[\text{S}_2\text{C}_2(\text{CF}_3)_2]_3\}^{2-}$ anion results from crystal packing forces.

Conclusions

Metal tris(dithiolene) complexes have been shown to be useful nonplanar building blocks for the preparation of magnetic electron-transfer salts. Magnetic measurements on $[\text{Fe}(\text{C}_5\text{Me}_5)_2]^{+}\{\text{Mo}[\text{S}_2\text{C}_2(\text{CF}_3)_2]_3\}^-$ provide evidence for weak ferromagnetic interactions, i.e., $\theta > 0$. This presumably arises from coupling between localized spins on adjacent anions and cations within the linear chains. On the basis of the field dependence of the magnetic susceptibility, however, bulk ferromagnetic behavior is not observed. The steric interactions between the peripheral CH_3 and CF_3 groups on adjacent molecules within the chains prevent good orbital mixing and therefore limit the strength of the intrachain coupling, while the peripheral substituents on the $\{\text{Mo}[\text{S}_2\text{C}_2(\text{CF}_3)_2]_3\}^-$ anion preclude the possibility of favorable $\text{D}^{\bullet+}/\text{A}^{\bullet-}$ interactions between chains. In light of these results, efforts are being directed toward preparation of analogous electron-transfer salts using radical anion complexes incorporating ligands with reduced steric demands and polarizable peripheral substituents.

Acknowledgment. We thank the Science and Engineering Research Council of Great Britain for a postdoctoral fellowship (W.B.H.) and C. Vazquez, W. Marshall, and R. S. McLean of DuPont for synthetic, crystallographic, and Faraday susceptibility assistance, respectively.

Supplementary Material Available: Summary of crystal data and collection parameters, interatomic distances and angles, least-squares planes, H-atom positions, and anisotropic thermal parameters for $[\text{Fe}(\text{C}_5\text{Me}_5)_2][\text{Mo}[\text{S}_2\text{C}_2(\text{CF}_3)_2]_3]$ and $[\text{Fe}(\text{C}_5\text{Me}_5)_2][\text{Mo}[\text{S}_2\text{C}_2(\text{CF}_3)_2]_3]$ (24 pages); tables of observed and calculated structure factors for $[\text{Fe}(\text{C}_5\text{Me}_5)_2][\text{Mo}[\text{S}_2\text{C}_2(\text{CF}_3)_2]_3]$ and $[\text{Fe}(\text{C}_5\text{Me}_5)_2][\text{Mo}[\text{S}_2\text{C}_2(\text{CF}_3)_2]_3]$ (36 pages). Ordering information is given on any current masthead page.

(33) Martin, J. L.; Takats, J. *Inorg. Chem.* 1975, 14, 1358.

Molecular Level Ceramic/Polymer Composites. 1. Synthesis of Polymer-Trapped Oxide Nanoclusters of Chromium and Iron

Manish Nandi,^{1a} Jeanine A. Conklin,^{1a} Lawrence Salvati, Jr.,^{1b} and
Ayusman Sen^{*,1a}

Chandlee Laboratory, Department of Chemistry, The Pennsylvania State University,
University Park, Pennsylvania 16802, and Perkin-Elmer Physical Electronics Laboratory,
Edison, New Jersey 08820

Received June 14, 1990

$\text{Cr}(\text{C}_6\text{H}_6)_2$ or $\text{Fe}_3(\text{CO})_{12}$ was added to polyamic acid solutions derived from 4,4'-oxydianiline and either 1,2,4,5-benzenetetracarboxylic acid dianhydride or 3,3',4,4'-benzophenonetetracarboxylic acid dianhydride. Following thermal curing, polyimide films containing a homogeneous dispersion of nanoclusters (size <1-1.5 nm) of Cr_2O_3 or $\alpha\text{-Fe}(\text{O})(\text{OH})$ were obtained. Both scanning electron microscopy and secondary ion mass spectroscopy depth profile indicated that the usually observed migration of the dopant to the polymer surface had not occurred. The chemical composition of the dopants were established by X-ray photoelectron spectroscopy.

The demand for materials with novel combinations of properties has led to the recent efforts in modification of

known polymers via the incorporation of a variety of additives. Ceramic nanoclusters with sizes ranging from <1

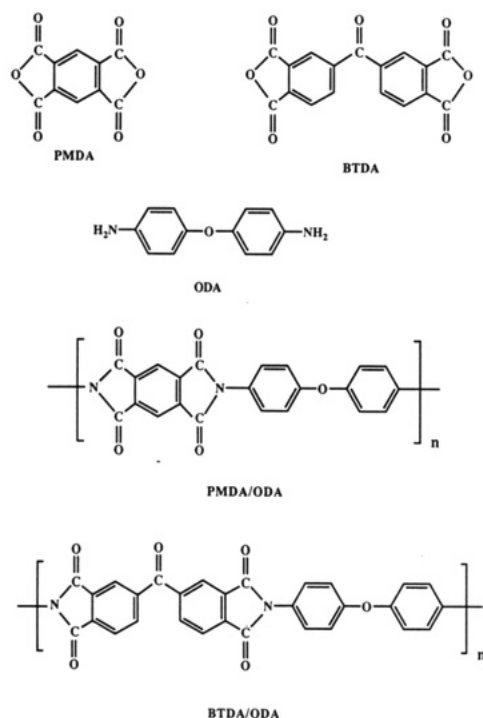


Figure 1. Chemical structures of the monomers and polymers.

to 10 nm represent a new class of materials with new properties that are different from those of discrete molecules, as well as bulk solid-state materials.² Their anticipated applications range from cluster-size dependant catalysis³ to nonlinear optics.⁴ In many of these applications, the ability to form films and fibers is an important requirement. This is most easily achieved by forming composites in which nanoclusters are embedded in a processable polymer matrix. A further advantage of synthesizing such composite is that the polymer matrix will physically prevent the agglomeration of the clusters—a persistent problem in size-selective cluster synthesis.

Aromatic polyimides have long been the material of choice in industry because of their high thermal stability, chemical resistivity, and mechanical strength.⁵ It was, therefore, of interest to see if ceramic nanoclusters could be formed in a polyimide matrix. The high glass-transition temperatures (T_g) of polyimides would be expected to further stabilize the nanoclusters by decreasing their mobility, thereby preventing their agglomeration to larger clusters. In our initial studies we have chosen to make chromium and iron oxide clusters because of their expected interesting magnetic and electronic properties.⁶



Figure 2. Photographs of free-standing polymer films of BTDA-ODA, PMDA-ODA/Cr, and BTDA-ODA/Fe.

Table I. Composition and Thermal Analyses of the Ceramic/Polymer Composites

polymer	metal wt %	metal mol %	TGA, °C	T_g , °C
PMDA-ODA			551	346
PMDA-ODA/Cr	2.9	20.0	513	333
PMDA-ODA/Fe	1.4	8.9	522	385
BTDA-ODA			545	361
BTDA-ODA/Cr	2.14	18.7	511	332
BTDA-ODA/Fe	0.95	7.7	536	351

^a 10% loss in weight of polymer. ^b Obtained from DSC experiments.

The formation of metal oxide containing polyimides by the incorporation of metal salts into the precursor polyamic acid prior to curing has been reported.⁷ However, a nonhomogeneous distribution of the oxide particles with markedly higher concentration at or near the polymer surface was often observed. In addition, large particles with sizes >100 nm are formed. In our approach to the synthesis of polymer-trapped nanoclusters, we have used the concept of "site isolation". The basic idea is to syn-

(1) (a) The Pennsylvania State University. (b) Perkin-Elmer Physical Electronics Laboratory.

(2) (a) Andres, R. P.; Averbach, R. S.; Brown, W. L.; Brus, L. E.; Goddard, W. A.; Kaldor, A.; Louie, S. G.; Moscovits, M.; Percy, P. S.; Riley, S. J.; Siegel, R. W.; Spaepen, F.; Wang, Y. *J. Mater. Res.* **1989**, *4*, 704. (b) Steigerwald, M. L.; Brus, L. E. *Annu. Rev. Mater. Sci.* **1989**, *19*, 471. (c) Brus, L. E. *J. Phys. Chem.* **1986**, *90*, 2555.

(3) (a) Kaldor, A.; Cox, D. M.; Zakin, M. R. In *Molecular Surface Chemistry: Reactions of Gas-Phase Metal Clusters*; Advances in Chemical Physics; Prigogine, I., Ed.; Wiley: New York, 1988; Vol. 70, Part 2, p 211. (b) St. Pierre, R. J.; El-Sayed, M. A. *J. Phys. Chem.* **1987**, *91*, 763.

(4) (a) *Nonlinear Optics of Organics and Semiconductors*; Kobayashi, T., Ed.; Springer-Verlag: Berlin, 1989; Part II. (b) Wang, Y.; Herron, N.; Mahler, W.; Suna, A. *J. Opt. Soc. Am. B* **1989**, *6*, 808. (c) Cheng, L.-T.; Herron, N.; Wang, Y. *J. Appl. Phys.* **1989**, *66*, 3417. (d) Jain, R. K.; Lind, R. C. *J. Opt. Soc. Am.* **1983**, *73*, 647.

(5) (a) *Polyimides: Synthesis, Characterization and Applications*; Mittal, K. L., Ed.; Plenum: New York, 1986. (b) Bessonov, M. I.; Koton, M. M.; Kudryavtsev, V. V.; Laius, L. A. *Polyimides*; Consultants Bureau: New York, 1987.

(6) A search performed by Chemical Abstracts Service (1977-90) yielded 158 and 2845 references, respectively, on the electronic and magnetic properties of Cr_2O_3 and Fe_2O_3 .

(7) Recent references: (a) Otsuka, I.; Shinada, T.; Mitshuboshi, M.; Inoue, H. *Jpn. Kokai Tokkyo Koho*; Japanese Patent 63,182,361, 1989; CA 110116226x. (b) Yamamoto, H.; Doi, T.; Ozawa, S. *Jpn. Kokai Tokkyo Koho*; Japanese Patent 63,172,741, 1989; CA 110155731c. (c) Porta, G. M.; Rancourt, J. D.; Taylor, L. T. *Chem. Mater.* **1989**, *1*, 269. (d) Rancourt, J. D.; Porta, G. M.; Moyer, E. S.; Madeleine, D. G.; Taylor, L. T. *J. Mater. Res.* **1988**, *3*, 996. (e) Boggess, R. K.; Taylor, L. T. *J. Polym. Sci., Poly. Chem. Ed.* **1987**, *25*, 685. (f) Taylor, L. T. In *Proceedings of the Second International Conference on Polyimides*; Society of Plastic Engineers: Ellenville, NY, 1985; p 351. (g) Rancourt, J. D.; Boggess, R. K.; Taylor, L. T. In *Proceedings of the Second International Conference on Polyimides*; Society of Plastic Engineers: Ellenville, NY, 1985; p 372. (h) Ezzell, S. A.; Taylor, L. T. *Macromolecules* **1984**, *16*, 1672. (i) Ezzell, S. A.; Furttsch, T. A.; Khor, E.; Taylor, L. T. *J. Polym. Sci., Poly. Chem. Ed.* **1983**, *21*, 865. (j) Furttsch, T. A.; Taylor, L. T.; Fritz, T. W.; Fortner, G.; Khor, E. *J. Polym. Sci., Poly. Chem. Ed.* **1982**, *20*, 1287. (k) Khor, E.; Taylor, L. T. *Macromolecules* **1982**, *15*, 379. (l) Ohmura, K.; Shibasaki, I.; Kimura, T. Japanese Patent 79,143,462, 1979; CA 92130214b.

thesize and maintain the clusters in isolated pockets in the polymeric matrix, and we achieve this by prebinding an organometallic precursor to specific sites on the polymer backbone. As described below, we have synthesized molecular level ceramic/polymer composites containing a homogeneous distribution of nanoclusters of chromium and iron oxides in polyimide matrices using this approach.

Results

The polymers chosen for our studies have structures depicted in Figure 1 (ODA = 4,4'-oxydianiline; PMDA = 1,2,4,5-benzenetetracarboxylic acid dianhydride; BTDA = 3,3',4,4'-benzophenonetetracarboxylic acid dianhydride). Upon curing to the fully imidized polymer, both PMDA-ODA and BTDA-ODA formed free-standing transparent golden-yellow films (Figure 2). In the case of the doped polymers, the initial homogeneous solution containing the organometallic precursor and the polyamic acid was green for chromium and wine red for iron. After being cured, the chromium-containing polymers formed free-standing transparent yellow-brown films (Figure 2). Similarly, the iron-containing films were also transparent but a little lighter in color (Figure 2). No discernible changes in flexibility and brittleness of the films were observed on doping.

The presence of dopants in the polymer matrix did not have a dramatic effect on their thermal properties (Table I). Thermogravimetric analysis in N_2 indicated that the polymer decomposition temperature, corresponding to 10% weight loss of the sample, decreased upon doping, with chromium showing a bigger effect than iron. We note that a decrease in polymer decomposition temperature has also been reported for other metal oxide containing polyimides, and the results suggest the presence of a metal-assisted decomposition pathway for the doped polymers.⁸ With respect to the glass transition temperature (T_g), differential scanning calorimetry (DSC) analysis did not reveal a consistent trend. However, since polyimides do not display a sharp glass transition point, the values reported in Table I are of limited accuracy.

The IR spectra of the doped polymers showed no evidence for any chemical interaction between the dopant and the polyimide matrix. The ^{13}C CP/MAS NMR of the chromium-containing polymers did not show any change in the ring resonances of the polyimides. Since any metal-arene interaction would result in upfield shifts of these resonances, such an interaction is evidently absent in the cured polymers. The carbonyl resonances are similarly unaffected. These observations, however, should be treated with caution. Since the molar ratios of metal to polymer repeating unit are low (Table I), subtle changes in the polymer may remain undetected by these techniques, especially in view of the broadness of the peaks.

The energy-dispersive X-ray analysis of the surfaces of the doped polymer films showed intense Cr and Fe peaks on both the atmosphere and the substrate sides. An X-ray dot mapping of Fe on the atmosphere side of the PMDA-ODA/Fe film revealed a uniform distribution of the metal throughout the surface of the films (Figure 3). A similar homogeneous distribution of Cr was also observed in the PMDA-ODA/Cr film. Although these observations indicate the presence of metal species at the polymer surface, scanning electron microscopy (SEM) of both the chromium- and iron-containing polymers showed uniform surfaces with no apparent microstructure, on both the

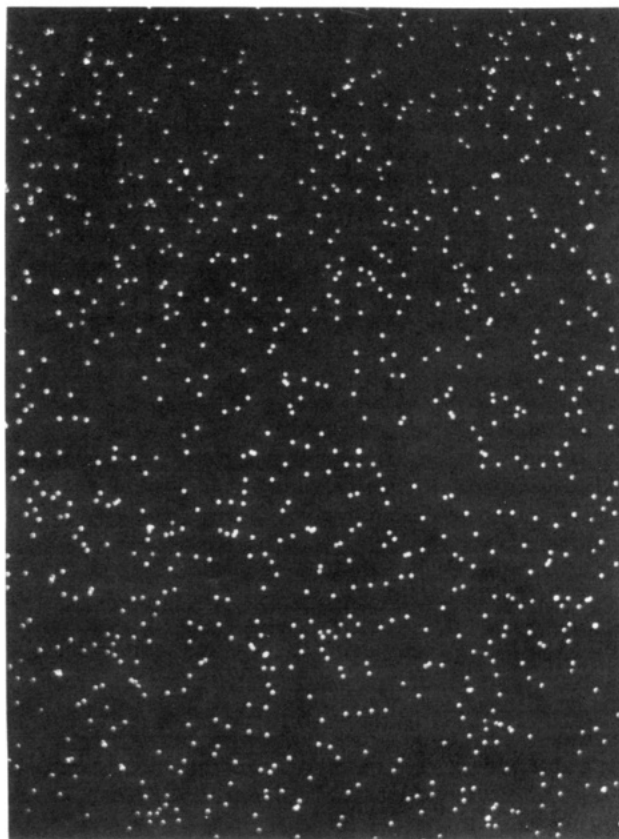


Figure 3. X-ray dot map of PMDA-ODA/Fe. The dots represent concentrations of Fe atoms.

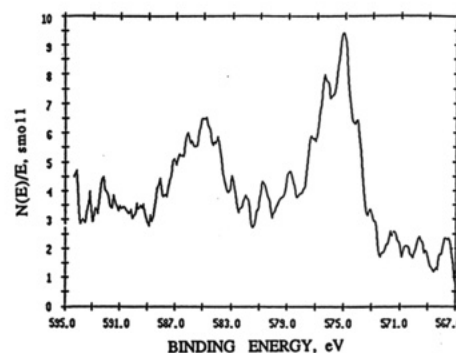


Figure 4. Chromium($2P_{1/2,3/2}$) photopeak region of the atmosphere side of PMDA-ODA/Cr.

atmosphere and the substrate sides of the films. In contrast to most previous reports on polyimides doped with metal compounds,⁷ no metal-containing aggregates were observed by SEM even at a magnification of 60 000. Clearly, neither the formation of a "metallic surface" nor a significant migration of any metal species to the film surfaces had occurred⁷ (also see the SIMS results).

The ESR spectrum of the PMDA-ODA/Cr showed a single resonance at $g = 2.018$, indicating the presence of an oxidized, paramagnetic chromium species.⁹ Further characterization of both the chromium and the iron species present in the PMDA-ODA polymeric matrix was achieved by X-ray photoelectron spectroscopy (XPS). XPS of the polymer films obtained at a takeoff angle of 90° for maximum sampling depth showed well-defined Cr(2p) and Fe(2p) on the atmosphere sides of the films. In the case of the PMDA-ODA/Cr, the Cr($2p_{3/2}$) peak was observed

(8) (a) Reference 7c. (b) Khor, E.; Taylor, L. T.; *Metal-Containing Polymer Systems*; Sheats, J. E., Carraher, Jr., C. E., Pittman, Jr., C. U., Eds.; Plenum: New York, 1985; p 367.

(9) Abragam, A.; Bleaney, B. *Electron Paramagnetic Resonance of Transition Ions*; Oxford University Press: London, 1970; p 432.

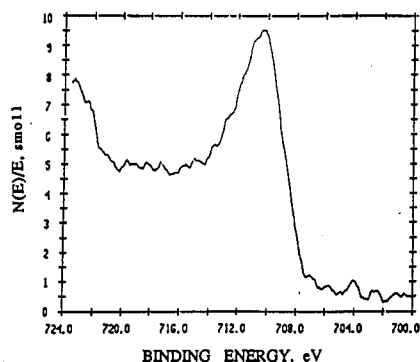


Figure 5. Iron($2P_{1/2,3/2}$) photopeak region of the atmosphere side of PMDA-ODA/Fe.

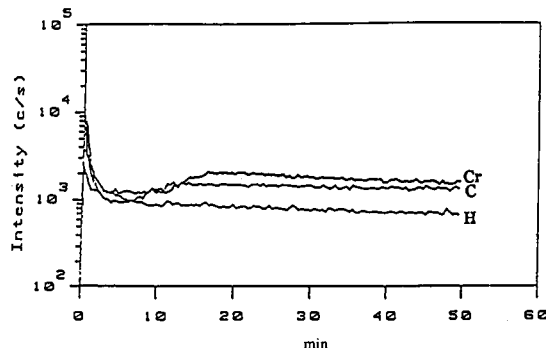


Figure 6. Depth profile of BTDA-ODA/Cr film (C, H, and Cr) by secondary ion mass spectroscopy (SIMS).

at a binding energy of 576.7 eV (Figure 4). This corresponded to the presence of Cr_2O_3 .¹⁰ The O(1s) photopeak at approximately 532 eV also suggested the presence of metal oxides.¹¹ The Fe($2p_{3/2}$) photopeak in PMDA-ODA/Fe was at 711.6 eV (Figure 5) and corresponded to the α -form of Fe(O)(OH).¹² It should be noted that although the formulation of Cr_2O_3 and α -Fe(O)(OH) is consistent with the XPS data, alternative combinations of oxo and hydroxo ligands cannot be totally ruled out. The XPS of the substrate sides of the films showed no detectable amounts of the metals.

The concentration gradient of the metal species in the BTDA-ODA films was studied by secondary ion mass spectroscopy (SIMS). A semiquantitative depth profiling from the atmosphere side of the films indicated that, for both the chromium- and iron-containing films, the concentration of the metal species increased slightly on going from the surface to the bulk and then leveled off (Figures 6 and 7). Thus, the combination of XPS and SIMS results indicates a near-homogeneous distribution of metal oxide clusters throughout the polyimide films except near (0–75 Å) the substrate-side surface, where no metal was detected (similar narrow metal-free zones near the substrate-side surface have been observed previously¹³ and has been ascribed to a zone-refining effect brought on by temperature gradients). Our results are in sharp contrast to the previous reports where the migration of the metal species from the bulk to the surface of the polymers was often observed (vide infra).⁷

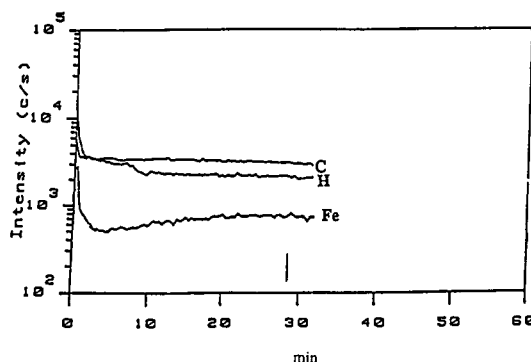


Figure 7. Depth profile of BTDA-ODA/Fe film (C, H, and Fe) by secondary ion mass spectroscopy (SIMS).

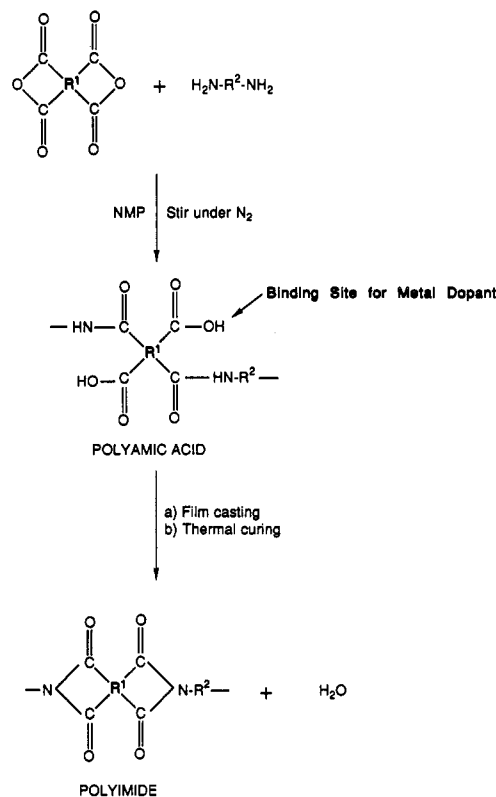


Figure 8. Steps involved in the synthesis of polyimide.

Finally, to probe the internal structure of the polymers, ultramicrotomed cross sections of the polymeric films were examined by transmission electron spectroscopy (TEM). The bulk of the films was found to be perfectly homogeneous, and no metal-containing species were detected. Thus, both SEM and TEM indicate that the size of the metal oxide particles present in the polymeric matrices is less than 1–1.5 nm, the resolution limit of the instruments.

Discussion

The spectroscopic studies on the polyimide films indicate the formation of a homogeneous dispersion of metal oxide (Cr_2O_3 or α -Fe(O)(OH)) nanoclusters (size <1.5 nm) in the polymers. These composite materials differ in two respects from previously synthesized metal oxide containing polyimides.⁷ The latter materials usually exhibit a nonhomogeneous distribution of the oxide particles with markedly higher concentration at or near the polymer surface. In addition, large particles with sizes >100 nm are present. We tentatively ascribe this difference to our use of zerovalent organometallic species (rather than metal salts) as precursors to the metal oxides. The zerovalent

(10) Carver, J. C.; Schweitzer, G. K.; Carlson, T. A. *J. Chem. Phys.* 1972, 57, 973.

(11) *Handbook of X-Ray Photoelectron Spectroscopy*; Wagner, C. D., Riggs, W. M., Davis, L. E., Moulder, J. F., Muilenberg, G. E., Eds.; Perkin-Elmer Physical Electronics Division: Eden Prairie, MN, 1979; pp 42–43.

(12) McIntyre, N. S.; Zetaruk, D. G. *Anal. Chem.* 1977, 49, 1521.

(13) Kim, Y.-H.; Kim, J.; Walker, G. F.; Feger, C.; Kowalczyk, S. P. *J. Adhesion Sci. Technol.* 1988, 2, 95.

organometallic species are readily oxidized¹⁴ and, as a result, lose their π -acid ligands (arene or CO) due to reduced metal-to-ligand back-bonding.¹⁵ Thus, upon oxidation binding of the metal to donor groups on the polymer backbone (e.g., the carboxylic acid groups in polyamic acid,¹³ Figure 8) is expected. In addition, the chromium may bind to the arene rings on the polymer backbone through the well-known arene-exchange reaction.¹⁶ We believe that this prebinding of the metal to the polymer backbone prior to the conversion to the oxide prevents (a) the migration of the metal species to the polymer surface and (b) the agglomeration to large oxide particles.

The source of oxygen for the metal oxides is the water formed during the polyamic acid-polyimide transformation. The evidence for this is as follows. The metal oxides were also formed when the curing was done in a nitrogen atmosphere. For both metals a limiting molar ratio of metal oxide to polymer repeating unit was invariably reached even with higher loadings of organometallic precursors. The limiting value (1:5 for Cr and 1:10 for Fe) did not change on going from PMDA-ODA to BTDA-ODA. This is not unexpected since both polyimides would yield 1 equiv of water per repeating unit upon curing. *A metal oxide to polymer repeating unit ratio that exceeded the above limiting value could be achieved only by deliberate addition of water to the polyamic acid-organometallic precursor mixture prior to curing.* In this way PMDA-ODA/Cr films containing 9.1% Cr (molar ratio of Cr to PMDA-ODA repeating unit 1:1) were obtained. Unfortunately a serious deterioration of film quality (e.g., loss of flexibility and mechanical strength) was observed with such high metal oxide loadings.

Experimental Section

Reactants and Solvents. The monomers used to synthesize the polyimides were 1,2,4,5-benzenetetracarboxylic acid dianhydride (PMDA), 3,3',4,4'-benzophenone tetracarboxylic acid dianhydride (BTDA), and 4,4'-oxydianiline (ODA). All the monomers were obtained from Aldrich Chemical Co. The chemical structures of the monomers are shown in Figure 1. PMDA and BTDA were purified by sublimation at 200 and 150 °C under 10⁻³ mmHg pressure, respectively. ODA was also purified by sublimation at 150 °C under a pressure of 10⁻³ mmHg. (Dibenzene)chromium was obtained from Alfa Chemical Co. and was used without further purification. Triiron dodecacarbonyl [Fe₃(CO)₁₂] was obtained from Strem Chemicals and was used without further purification. All chemicals, once purified, were stored in N₂-filled glovebox. Anhydrous *N*-methylpyrrolidinone (NMP) was obtained from Aldrich Chemical Co. and was stored under nitrogen.

Synthesis of Polymer Precursors. The polyimide precursor, poly(amic acid), was synthesized by the reaction of the appropriate dianhydride and the diamine in NMP (10–15% solids).

In a typical synthesis, the diamine, ODA (1.0 g, 0.005 mol), was placed in a 50-mL glass flask, and the appropriate amount of the solvent (NMP) was added to it. The dianhydride, PMDA (1.079 g, 0.00495 mol), was then added to the solution after complete dissolution of the diamine. The mixture was stirred mechanically

for 10–12 h to form a golden-yellow polyamic acid solution.

To synthesize the precursors to the modified polymers, Cr-(C₆H₆)₂ (0.26 g, 0.00125 mol) or Fe₃(CO)₁₂ (1.26 g, 0.0025 mol) was added to the polyamic acid solution at this point. The solution then was stirred again for 10–12 h under nitrogen to form a homogeneous metal precursor/poly(amic acid) solution.

Polymer Curing and Film Preparation. The polymer films (approximately 0.05 mm in thickness) were prepared by casting either the poly(amic acid) solution or the metal precursor/poly(amic acid) solution on a glass plate under a dust-free nitrogen atmosphere. All glass plates were cleaned by ultrasonication in hexane and then by washing with doubly deionized water. The polymers were then thermally cured by heating under dry nitrogen at 100 °C for 1 h, 150 °C for 1 h, 200 °C for 1 h, and finally at 300 °C for 1–2 h. After cooling down to room temperature, the high quality free-standing films were easily removed by soaking them in deionized water and peeling off with a razor blade. All the polymer films were finally cleaned by ultrasonication in acetone and hexane. They were then dried in a vacuum oven for 30 min at 140 °C. IR spectra indicated that polyimide-poly(amic acid) reconversion had not occurred on treatment with water.

Characterization of Polymers. Infrared spectra were obtained with Perkin-Elmer FT-IR 1710 instrument. ¹³C CP/MAS NMR spectra were obtained by using a Chemagnetics CMC-300A (300 MHz) operating at a resonance frequency of 74.9 MHz for the carbon-13 nucleus. All elemental analyses including metals were done at Galbraith Laboratories, Knoxville, TN.

A Du Pont Thermal Analyst 2100 system was used for the thermogravimetric analysis. The samples were heated at the rate of 10 °C/min from room temperature to 1000 °C under a flow of dry N₂ at 10 mL/min. Differential scanning calorimetric experiments were carried on a Perkin-Elmer DSC 7 heating at a rate of 20 °C/min from room temperature to 450 °C under N₂.

Scanning electron micrograms (SEM) were taken on a International Scientific Instruments Model DS130 scanning electron microscope. All samples were gold coated and mounted on aluminum mounts with silver cement. Energy-dispersive X-ray analysis and X-ray dot mapping were done with a Kevex 8000 system.

Transmission electron micrograms (TEM) were obtained by using a Philips 300 transmission electron microscope. Samples were prepared by embedding small strips of polymer films in Spurr¹⁷ media, which were then polymerized at 70 °C overnight. Samples were sectioned to 500 Å by using a dry glass knife mounted on a LKB Ultratome III. Care was taken to cut the cross sections perfectly straight so as not to have blurred edges on the polymer film strips. The thin sections were placed on a 200-mesh copper grid for analysis.

Secondary ion mass spectroscopy (SIMS) was done with a CAMECA IMS-3F instrument using a 17-kV ¹⁸O⁻ electron gun. A sample of 80 nA was spread over 250 × 250 μm area, and analysis was done from a 60-μm-diameter area at the center.

X-ray photoelectron spectra were obtained with a Perkin-Elmer PHI Model 5000LS ESCA system. A monochromatic X-ray source with an aluminum anode (Al Kα = 1486.7 eV) run at 600 W (15 kV and 40 mA) was used. The analysis area was set at 1.1 mm, and the takeoff angles used were 43° and 90°. The data were examined for differential charging effects, and none was found. All binding energies were referenced to the aromatic C(1s) photopeak at 284.6 eV.

Acknowledgment. This research was supported by a grant from the U.S. Department of Energy, Office of Basic Energy Sciences (DE-FG02-84ER13295).

Registry No. (PMDA)(ODA) (copolymer), 25038-81-7; (PMDA)(ODA) (SRU), 25036-53-7; (BTDA)(ODA) (copolymer), 24980-39-0; (BTDA)(ODA) (SRU), 24991-11-5; Cr(C₆H₆)₂, 1271-54-1; Fe₃(CO)₁₂, 17685-52-8.

(14) (a) Davis, R.; Kane-Maguire, L. A. P. *Comprehensive Organometallic Chemistry*; Wilkinson, G., Stone, F. G. A., Abel, E. W., Eds.; Pergamon: New York, 1982; Vol. 3, p 999. (b) Shriver, D. F.; Whitmire, K. H. *Comprehensive Organometallic Chemistry*; Wilkinson, G., Stone, F. G. A., Abel, E. W., Eds.; Pergamon: New York, 1982; Vol. 4, p 262.

(15) Collman, J. P.; Hegedus, L. S.; Norton, J. R.; Finke, R. G. *Principles and Applications of Organotransition Metal Chemistry*; University Science Books: Mill Valley, CA, 1987; p 43.

(16) Reference 14a, p 990.

(17) Spurr, A. R. *J. Ultrastructure Res.* **1969**, *26*, 31.